



different types of loading for PP, PE and PMMA. This comparison proved that MIR gives the prediction with an average error of 0.05%.

## **Notations**

$F_{ij}$	A non-linear tensile function
$t$	Time (s)
$e$	Strain
$I_1, I_2'$	Stress invariants
$K_1, K_2, K_3$	Hydrostatic, deviatoric and synergistic tensile kernel functions
$G_1, G_2$	Deviatoric shear kernel functions
$e_{11}$	Tensile strain
$e_{12}$	Shear strain
$n$	Time constant
PMMA	Polymethyl methacrylate
PE	Polyethylene
MIR	Multiple integral representation
PP	Polypropylene
$tr$	Trace
$v_0, \dots, v_3$ and $\pi_1, \dots, \pi_5$	Time functions including the material constant
$\tau$	Shear stress
$\xi$	Time parameter (s)
$\sigma$	Tensile stress (N/m <sup>2</sup> )
$I$	Unit matrix
$\sigma_{ij}$	Stress tensor
$e_{ij}$	Strain tensor

## **1. Introduction:**

Polymers are the fastest growing class of engineering materials in volume of usage and now firmly established in many load-bearing duties. The structure of polymers below glass transition is non-equilibrium inhomogeneous<sup>[1]</sup>, so that the stress and strain analysis is complicated<sup>[1, 2]</sup>. Also, the deformation behaviour of thermoplastics under mechanical loads

depends to a great extent on time. The influence of time makes the dimensioning of plastic components considerably more complicated than other materials<sup>[3]</sup>.

Different attempts of researchers investigated the creep behaviour of plastics from different sights. The first attempt to study the effect of hydrostatic ( $I_1$ ) and deviatoric ( $I_2'$ ) stresses was by Buckley and McCrum<sup>[4]</sup> whose found that the linear response of solid polymers is related to the hydrostatic stress while the non-linear response is related to the deviatoric stress. Resen<sup>[5]</sup> designed a biaxial creep machine and performed many experiments under tension, torsion and combined tension-torsion loading to study the separate roles of ( $I_1$ ) and ( $I_2'$ ). Also, for the same purpose, Jabbar<sup>[6]</sup> and Zai'bel<sup>[7]</sup> performed many experiments under combined tension-internal pressure and combined tension-torsion- internal pressure loading respectively. Also Za'ibel<sup>[7]</sup> proposed an analytical procedure by using the finite and boundary element formulations to predicate the onset of non-linear creep, recovery and stress relaxation. Oliveira and Creus<sup>[8]</sup> used a numerical method for modeling the failure behaviour of composite laminates in the presence of large displacements and creep. The modeling of material behaviour included thermal, and viscoelastic effects, using an efficient state variable representation. Thus, the procedure can be used to analyze buckling, creep, buckling and creep including damage. Then they have been extended this procedure to study the nonlinear viscoelasticity of thin-walled beams in composites materials<sup>[9]</sup> and ageing in fiber reinforced polymer composites<sup>[10]</sup>. Resen and Faisal<sup>[11]</sup> used MIR to predict the creep response of PMMA under combined tension-torsion loading. They found that MIR gives a good perdition for long term of creep under combined loading.

As we knew ( $I_1$ ) represents the components of the applied stresses which cause the linear response while ( $I_2'$ ) represents the components of the applied stresses which cause the nonlinear response. Until now MIR is depend on the applied stresses and don't use the stress invariants. Also most researches are limited to experimental study and to the linear and the onset of the nonlinear range. Thus, the aim of this work is to insert ( $I_1$ ) and ( $I_2'$ ) into the relations of MIR and predict the non-linear creep of semicrystalline and amorphous solid polymers which help us to separate the linear and nonlinear response and know to which range of strain we should be used these materials in engineering application.

## **2. Theory:**

### **2.1 Constitutive Relationship:**

The strain of polymeric materials can be expressed in the form of multiple integrals due to the dependency of the strain at any time on all stress history <sup>[2]</sup>.

$$e(t) = F_{ij} \left[ \frac{d\sigma(\xi)}{d\xi} \right]_{-\infty}^t \quad \dots(1)$$

where  $\sigma$  and  $e$  are the stress and strain tensors respectively,  $F_{ij}$  is a non-linear tensile function, and  $\xi$  is an arbitrary time.

This behaviour could be described by containing the stress terms up to third order. Thus, for the case of step loading, the strain tensor is given by the following equation becomes <sup>[2]</sup>:

$$e = I \left[ \pi_1 \text{tr} \sigma + \pi_2 \text{tr}(\sigma\sigma) + \pi_3 \text{tr} \sigma \text{tr} \sigma + \pi_4 \text{tr} \sigma \text{tr}(\sigma\sigma) + \pi_5 \text{tr} \sigma \text{tr} \sigma \text{tr} \sigma \right] + \left[ v_0 + v_1 \text{tr} \sigma + v_2 \text{tr}(\sigma\sigma) + v_3 \text{tr} \sigma \text{tr} \sigma \right] \sigma \quad \dots(2)$$

where  $e = e_{ij}$  is the strain tensor.

$\pi_i$  and  $v_j$  are the time functions including the material constant <sup>[2]</sup>.

$$i = 1, \dots, 5$$

$$j = 0, \dots, 3$$

tr = trace

## **2.2 Loading Programs:**

### **2.2.1 Uniaxial tensile loading:**

For this case of uniaxial tensile loading, the stress tensor and its traces are:

$$\sigma_{ij} = \begin{bmatrix} \sigma_{11} & 0 & 0 \\ 0 & 0 & 0 \\ 0 & 0 & 0 \end{bmatrix}, \quad \text{tr} \sigma = \sigma_{11}, \quad \text{tr} \sigma \sigma = \sigma_{11}^2 \quad \dots(3)$$

Where  $\sigma_{11} = \sigma$  and  $\sigma$  is the tensile stress.

Also, the stress invariants for this case is given by:

$$I_1 = \sigma_{11} \quad \dots(4a)$$

$$I'_2 = \frac{\sigma_{11}^2}{3} \quad \dots(4b)$$

Substituting Eqs. (3) and (4) into Eq. (2), the tensile strain  $e_{11}(t)$  can be obtained as follows:

$$\begin{aligned} e_{11}(t) &= \pi_1 I_1 + 3\pi_2 I'_2 + 3\pi_3 I'_2 + 3\pi_4 I_1 I'_2 + 3\pi_5 I_1 I'_2 + \\ &\quad \nu_0 I_1 + 3\nu_1 I'_2 + 3\nu_2 I_1 I'_2 + 3\nu_3 I_1 I'_2 \\ &= K_1 I_1 + K_2 I'_2 + K_3 I_1 I'_2 \end{aligned} \quad \dots(5)$$

Where  $K_1 = \pi_1 + \nu_0$

$$K_2 = 3 \times (\pi_2 + \pi_3 + \nu_1)$$

$$K_3 = 3 \times (\pi_4 + \pi_5 + \nu_2 + \nu_3)$$

Where  $K_1, K_2$  and  $K_3$  are the hydrostatic, deviatoric and synergistic tensile kernel functions respectively.

According to Eq. (5), three pure tension tests at different stress levels are required to determine the unknown kernels  $K_1, K_2$  and  $K_3$ .

### 2.2.2 Pure shear loading:

For this case, the stress tensor and its traces are given by the following equation:

$$\sigma_{ij} = \begin{bmatrix} 0 & \tau & 0 \\ \tau & 0 & 0 \\ 0 & 0 & 0 \end{bmatrix}, \quad \text{tr}\sigma = 0, \quad \text{tr}\sigma\sigma = 2\tau^2 \quad \dots(6)$$

Where  $\tau$  is the shear stress, but:

$$I_1 = 0 \quad \dots(7a)$$

$$I'_2 = \tau^2 \quad \dots(7b)$$

Substituting Eqs. (6) and (7) into Eq. (2), the shear  $e_{12}(t)$  strain can be obtained as follows:

$$\begin{aligned} e_{12}(t) &= (v_0 + 2v_2 I_2') \sqrt{I_2'} \\ &= G_1 \sqrt{I_2'} + G_2 (I_2')^{3/2} \end{aligned} \quad \dots(8)$$

Where  $G_1 = v_0$

$$G_2 = 2v_2$$

$G_1$  and  $G_2$  are the deviatoric shear kernel functions.

It can be noted (from Eq. (8)) that two pure shear tests at different stress levels are required to determine these unknown kernels.

### **3. Results and Discussion:**

#### **3.1 Uniaxial tensile loading:**

The behaviour of semicrystalline PE and PP at 20°C and amorphous PMMA at 30°C was studied over time range of 3, 30 and 3 hr respectively. The block diagram of the program which has been written is shown in Fig 1. The responses of three uniaxial tests at different stresses<sup>[5, 12]</sup> (Table 1) have been substituted into Eq. (5) to determine the hydrostatic  $K_1$ , deviatoric  $K_2$  and synergistic  $K_3$  tensile functions by using Guassin elimination. Then, least square method has been used for fitting these functions in terms of power law as given in Table 2. It was found that time exponents for PE, PP and PMMA are 0.125, 0.07 and 0.065 respectively which are similar to those found by Faisal<sup>[13]</sup>. These functions are presented in Fig. 2, 3 and 4.

Fig. 2 shows that  $K_1$  and  $K_2$  increase non-linearly with time while  $K_3$  decrease non-linearly with time. In contract Figs. 3 and 4 show that  $K_1$  and  $K_3$  increase non-linearly with time whereas  $K_2$  decreases non-linearly with time. These increasing or decreasing can be noted from the log scale of the time which depend on the type of material if it is amorphous or semicrystalline. The change is only in the behaviour of  $K_2$  and  $K_3$  which can be attributed to the decreasing of the degree of crystallization<sup>[2]</sup>.

Substituted these functions (Table 2) into Eq. (5) to find the tensile strains at different hydrostatic ( $I_1$ ) and deviatoric ( $I_2'$ ) stress level. These determined strains were compared with experimental results<sup>[5, 12]</sup> as shown in Figs. 5, 6 and 7. A good agreement between the experimental<sup>[5, 12]</sup> and MIR

results has been obtained with a tensile error of  $2.892835 \times 10^{-4}$ . From these figures it can be noted that tensile strain increase non-linearly with time and increasing of  $I_1$  and  $I_2'$  caused a step shift in these curves because  $I_1$  and  $I_2'$  depend on the applied stresses. Since  $I_2'$  depends on  $I_1$ , so this shift occurred due to increment in  $I_1$  that can be consider the main factor for the case of uniaxial tensile loading which agree with the results of Resen<sup>[5]</sup>.

### 3.2 Pure shear loading

For the case of pure shear loading, the behaviour of PMMA at 30°C was studied over the time range of 3 hr. by substituting the responses of two pure shear tests<sup>[5]</sup> at different stresses (Table 3) and by using block diagram of the program which is shown in Fig 1. The deviatoric shear functions  $G_1$  and  $G_2$  have been determine by using the same procedure that mentioned in section 3.1.

It was found that time exponent of these functions is the same as that found for the tensile functions of PMMA (Table 2). These functions are also present in Fig. 8, which indicate that both  $G_1$  and  $G_2$  are increase nonlinearly with time.

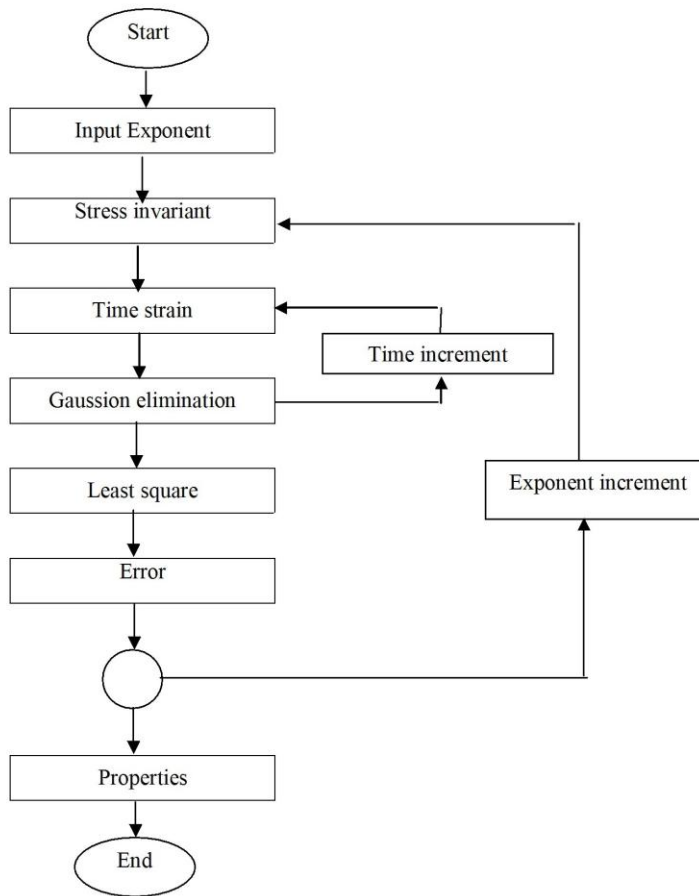
Substituting  $G_1$  and  $G_2$  into Eq. (8) to find the shear response at different values of  $I_2'$ . Fig. 9 shows the comparison between the experimental<sup>[5]</sup> and MIR results. A good agreement between these results has been obtained with a shear error of  $1.219314 \times 10^{-3}$ . Also it can be noted that the increasing of  $I_2'$  caused of step shift in the curves of shear strains, which indicate that  $I_2'$  is the main factor for the case of pure shear loading.

From the comparison shown in Figs. 5, 6, 7 and 9, it can be noted that a good agreement was obtained by using the formulation that derived in this paper. Also the total error in tensile and shear strains was 0.05%.

### 4. Conclusions:

New constitutive equations have been obtained by inserting  $I_1$  and  $I_2'$  into the MIR. For the case of uniaxial tensile, the functions have been obtained are the hydrostatic, deviatoric and synergistic functions for PE, PP and PMMA. While only the deviatoric functions have been obtained for the case of pure shear loading. Also it was found that tensile strain depends on  $I_1$  while shear strain in highly dependent on  $I_2'$ . The obtained error in the first case was  $2.892835 \times 10^{-4}$  and  $1.219314 \times 10^{-3}$  for the second case. The total error in tensile and shear strains was 0.05%.

**Fig. 1 The block diagram of MIR**



Main subroutine	Function
Stress invariants	To enter stresses ivariants date required for calculation of Gaussian elimination
Time, Strain	To enter time and a corresponding strain at stresses given in stress subroutine
Gaussian	To find kernel functions
Time increment	To control increments if time is intended to be in incermental form.
Least square	To find the kernel functions in the form of power law
Error	To calculate the error between the experimental and MIR results.
Properties	To obtain creep compliance and compressibility function in terms of power law. Also, to calculate their values and Poisson's ratio at any required time and stress.

Table 1 The hydrostatic and deviatoric stresses

that used to find  $K_1$ ,  $K_2$  and  $K_3$

<i>Material</i>	No. Of Test	$I_1$ (MPa)	$I_2$ (MPa <sup>2</sup> )
<b>PE</b>	1	0.5520	0.5071040
	2	1.1030	0.4055360
	3	1.6550	0.9130080
<b>PP</b>	1	1.3780	0.6326910
	2	4.1360	5.7021650
	3	6.8970	15.856203
<b>PMMA</b>	1	12.247	49.996336
	2	24.247	195.97200
	3	34.600	399.05300

**Table 2 Hydrostatic, deviatoric and synergistic tensile functions for different materials.**

<i>Material</i>	N	Tensile functions
<b>PE</b>	0.125	$K_1 = 0.1809797E-3 + 568.7743E-3 t^n$ $K_2 = 100.40550E-3 + 276.9348E-3 t^n$ $K_3 = 49.481490E-3 + 38.00241E-3 t^n$
<b>PP</b>	0.07	$K_1 = - 14.1241E-3 + 132.25400E-3 t^n$ $K_2 = 6.960681E-3 - 27.102280E-3 t^n$ $K_3 = -1.556835E-3 + 4.621695E-3 t^n$
<b>PMMA</b>	0.065	$K_1 = 0.52972650E-3 + 2.0826460E-3 t^n$ $K_2 = 0.70489650E-3 - 0.6110778E-3 t^n$ $K_3 = -0.03216576E-3 + .03867906E-3 t^n$

Table 3 Hydrostatic and deviatoric stresses that used to find  $G_1$  and  $G_2$  for PMMA.

<i>Material</i>	No. of Test	$I_1$ (MPa)	$I_2$ (MPa <sup>2</sup> )
<b>PMMA</b>	1	0	299.29
	2	0	49.985

**Table 4 Deviatoric shear functions for PMMA.**

Material	n	Shear functions
PMMA	0.065	$G_1 = 0.09663496E-3 + 0.26425420E-3 t^n$ $G_2 = -0.02205132E-3 + 0.02946145E-3 t^n$

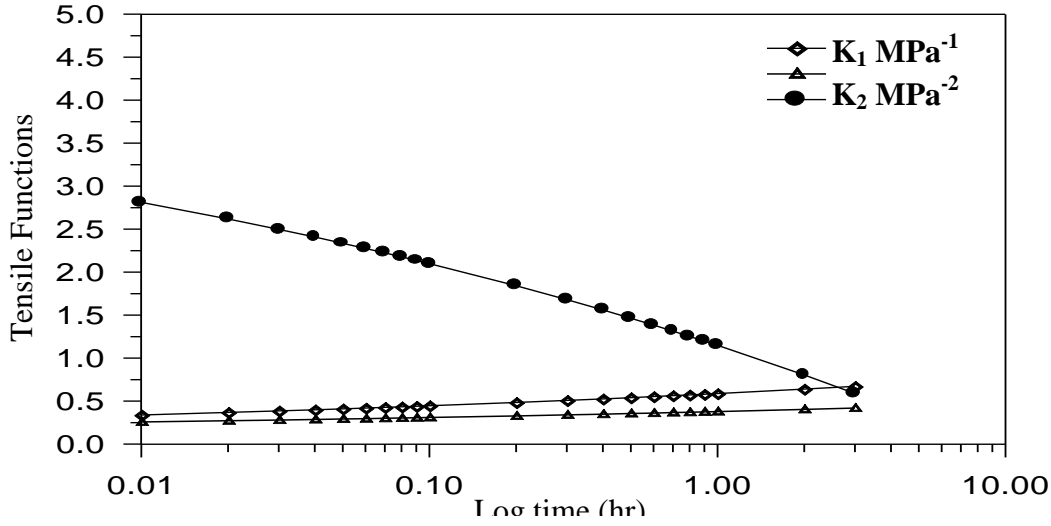


Fig. (2) Hydrostatic, deviatoric and synergistic tensile kernel functions of PM at 20°C

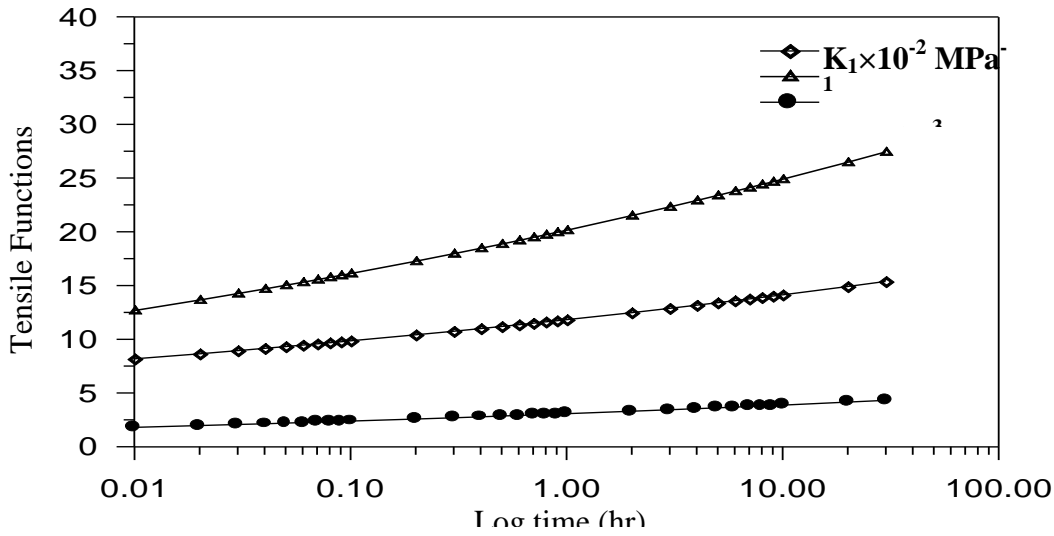


Fig. (3) Hydrostatic, deviatoric and synergistic tensile kernel functions of PP at 20°C

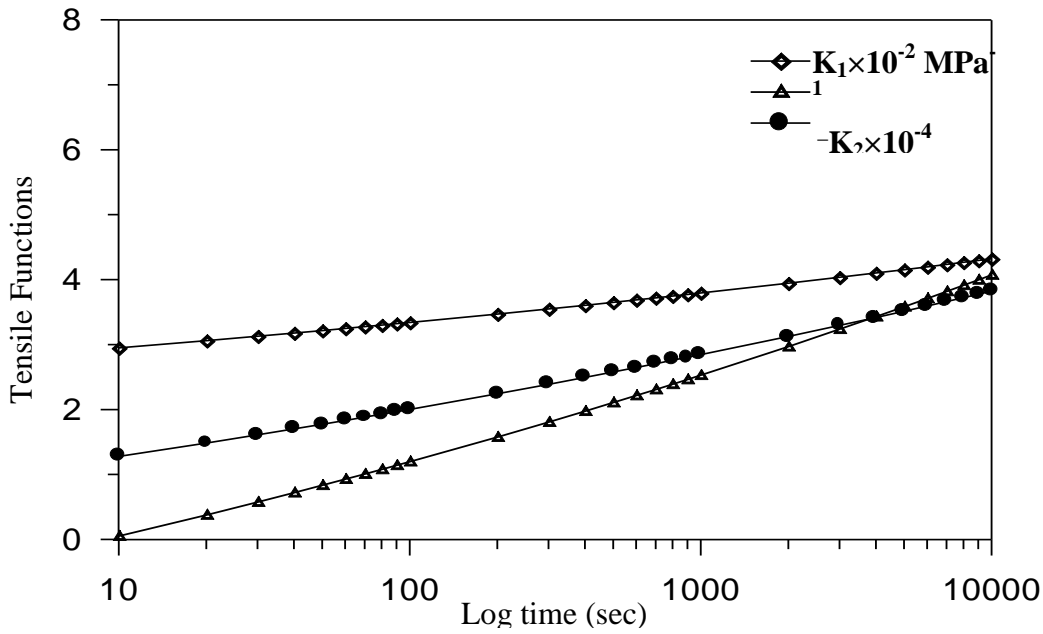


Fig. (4) Hydrostatic, deviatoric and synergistic tensile kernel functions of PMMA at 30°C.

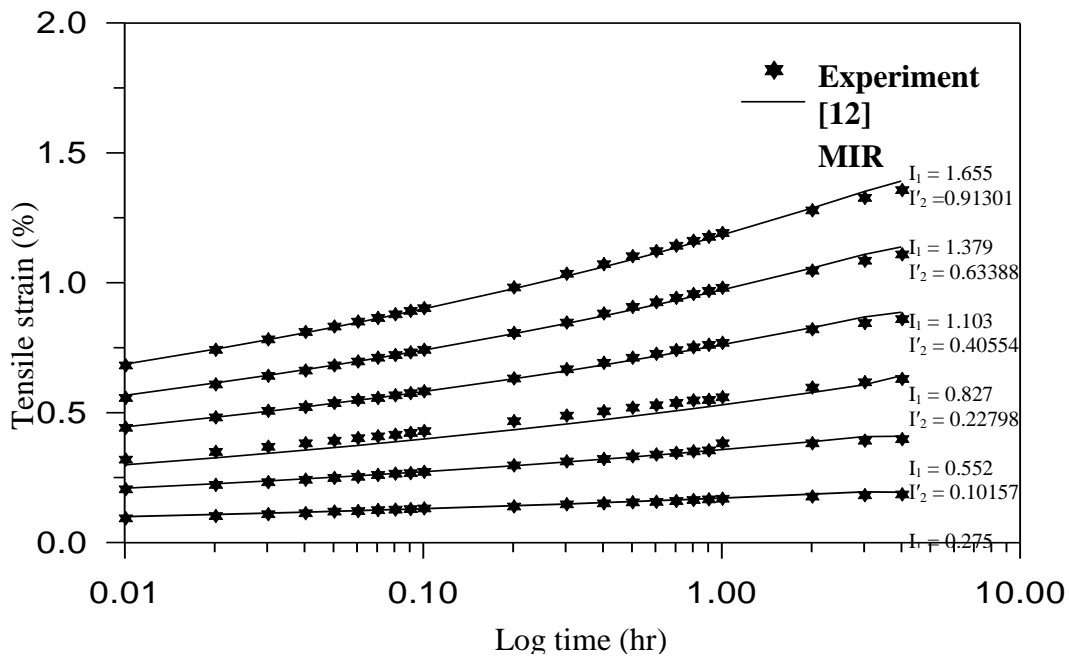


Fig. (5) Creep curves of PE for different hydrostatic and deviatoric stress at 20°C.

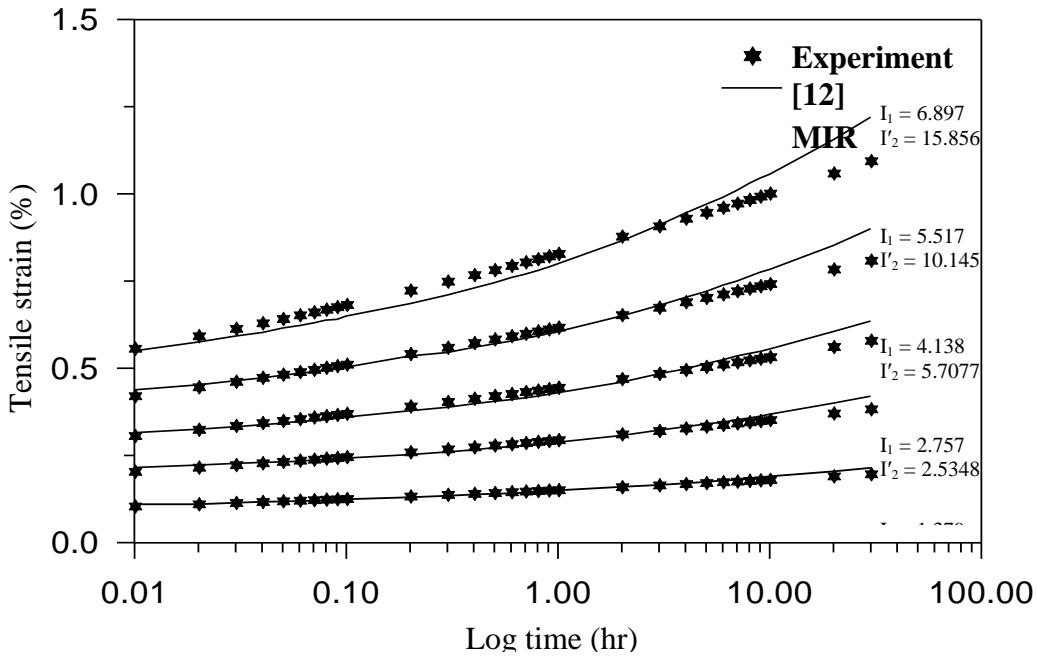


Fig. (6) Creep curves of PP for different hydrostatic and deviatoric stress at 20°C.

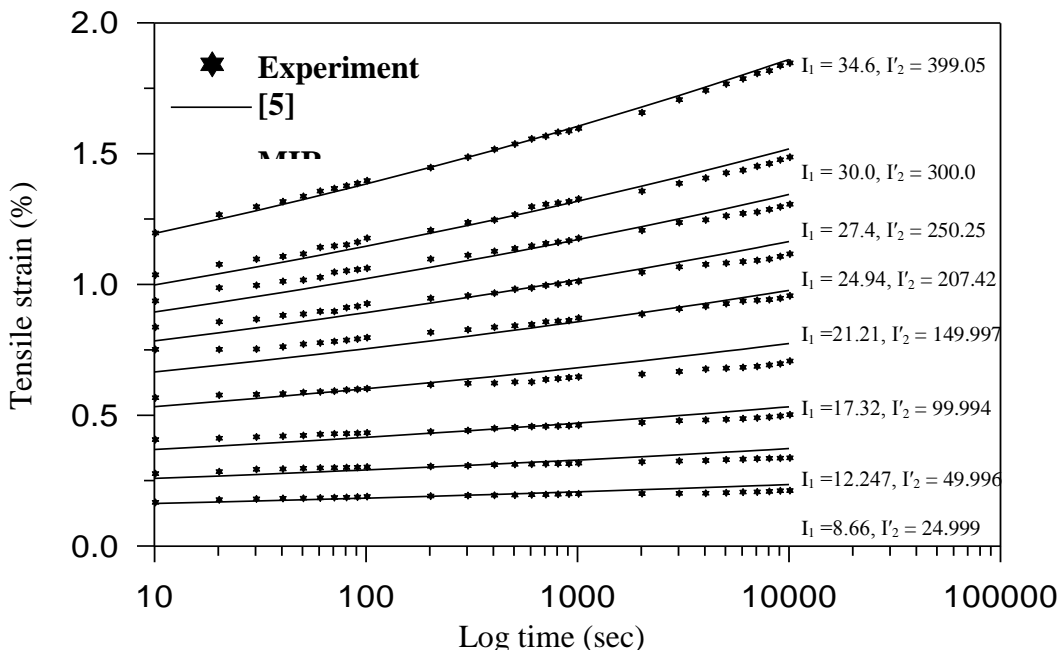


Fig. (7) Creep curves of PMMA for different hydrostatic and deviatoric stress at 30°C.

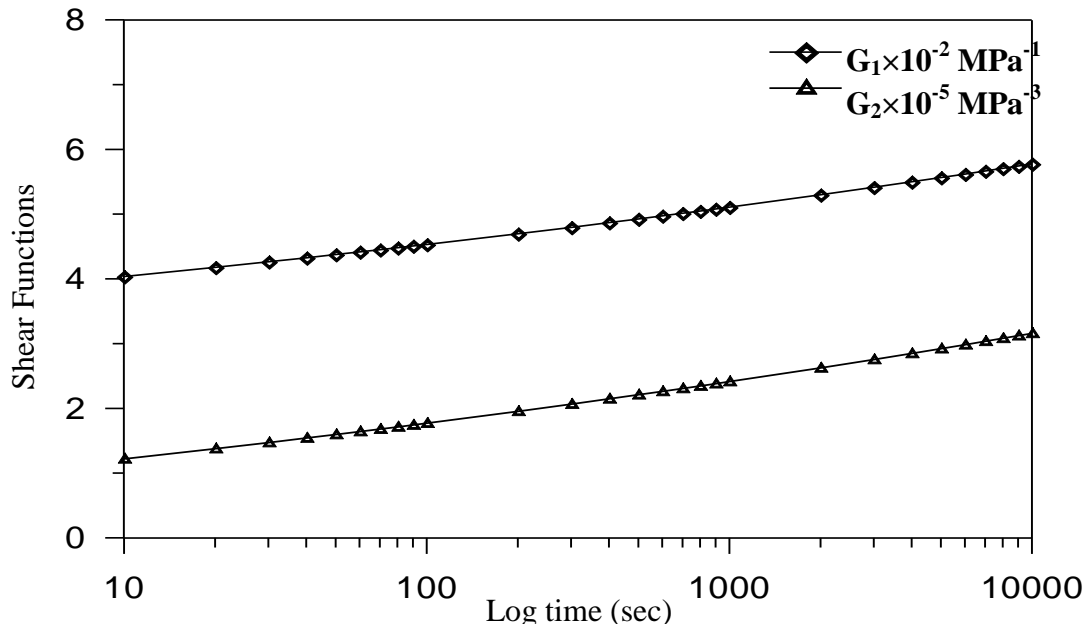


Fig. (8) Deviatoric shear kernel functions of PMMA at 30°C.

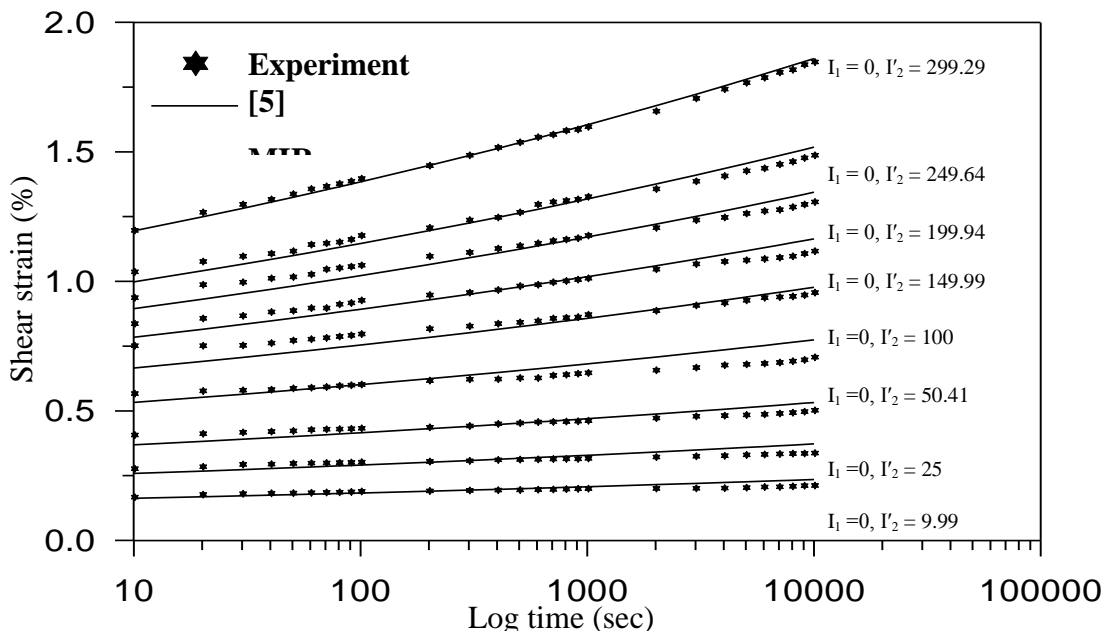


Fig. (9) Creep curves of PMMA for different hydrostatic and deviatoric stress at 30°C.

## **References:**

1. Robertson, m. E., "The theoretical and experimental investigation of non-linear viscoelasticity of glassy polymers", Ph. D. thesis, The Royhal institute of technology, Stockholm, Sweden, 1984.
2. Onaran, K., Findley, W. N., "Combined stress creep experiments on a non-linear viscoelastic material to determine the kernel functions for multiple integral representation of creep", Trans. Soci. Rheol., Vol 9., No. 2, PP. 229-327, 1965.
3. Resen, A. S., "Analytical expression for stress-strain curves of PMMA at different strain rates", Engg. Tech. J., Vol. 5, No. 1, PP. 147-159, 2001.
4. Buckley, C. P., McCrum, N. G., "The relation between linear and non-linear viscoelasticity of PP", J. Mater. Sci., Vol. 9, PP. 2064-2066, 1974.
5. Resen, A. S., "Biaxial creep of plastics", Ph. D. Thesis, The University of Manchester Institute of Science and Technology, England, 1988.
6. Jabbar, K. A., "Creep in plastics", M. Sc. Thesis, Mechanical Engineering department, University of Basrah, Basrah, Iraq, 1997.
7. Za'ibel, A. H., "Creep, Recovery and stress relaxation of plastics under combined load systems", Ph. D. Thesis, Mechanical Engineering department, University of Basrah, Basrah, Iraq, 1999.
8. Oliveira, B. F., Creus, G. J., "Viscoelastic failure analysis of composite plates and shells", Comps. Struc., Vol. 49, PP. 369-384, 2000.
9. Oliveira, B. F., Creus, G. J., "Nonlinear viscoelastic analysis of thin-walled beams in composite materials", Thin-walled Struc., Vol. 41, PP. 957-971, 2003.
10. Oliveira, B. F., Creus, G. J., "An analytical-numerical framework for the study of ageing in fibre reinforced polymer composite", Comps. Struc., Vol 65, PP. 443-457, 2004.
11. Resen, A. S., Faisal, B. M., "Multiaxial creep analysis of PMMA", Iraqi J. poly. , Vol. 5, No. 1, PP. (129-152), 2005.
12. Ogorkiewicz, R. M., "Engineering properties of thermoplastics", John Wiley & Sons Ltd., 1970.
13. Faisal, B. M., "The non-linear creep analysis in plastics using multiple integral representation", M. Sc. Thesis, Mechanical Engineering department, University of Basrah, Basrah, Iraq, 2000.

Recived ..... ( 11/5/2008 )

Accepted ..... ( 3/9 /2008 )